2009 International Symposium on Nonlinear Theory and its Applications
NOLTA'09, Sapporo, Japan, October 18-21, 2009

Possibility of logic operations in a micro-mechanical cantilever array

M. Sato†, Y. Nagata†, N. Fujita† and A. J. Sievers‡

†Graduate School of Natural Science and Technology, Kanazawa University
Ishikawa 920-1192, Japan
‡Laboratory of Atomic and Solid State Physics, Cornell University
Ithaca, NY 14853-2501, USA
Email: msato@kenroku.kanazawa-u.ac.jp

Abstract–We report on a possible method for realizing logic operations in a micro-mechanical cantilever array based on the timed application of a lattice disturbance to control the properties of intrinsic localized modes (ILMs). The application of a specific inhomogeneous field destroys a driver-locked ILM, while the same operation can create an ILM if initially no-ILMs exists. Logic states "1" and "0" correspond to "present" or "absent" ILMs.

1. Introduction

In a micromechanical array, a localized nonlinear excitation called an intrinsic localized mode (ILM) can be generated.[1] It is stable at a lattice site, and can be moved from one place to another by introducing a mobile impurity in the array. The interaction between an ILM and an impurity mode makes such motion possible. Because of damping such ILMs are usually driven by a cw oscillator to maintain constant amplitude and the oscillation frequency of the ILM is locked to the driver. So far, we have succeeded in seeding, annihilating, repelling and attracting driver-locked ILMs by using impurities.[1] Dynamic control is also possible using a soliton when two bands are available, one for ILMs and the other for the soliton.[2]

For a nonlinear array with hard nonlinearity a stationary ILM can be created above the band states. When an impurity mode frequency is above the band state frequencies but below the ILM frequency the ILM is attracted to it. (See Ref. 1, Fig. 9.) Two sets of frequency differences are important for the impurity control of the ILM. These are between the driver and the highest frequency pure-band state $\Delta_{dm} = \omega_d - \omega_m$ and the frequency difference between the driver and the impurity mode $\Delta_{di} = \omega_d - \omega_i$. Since the ILM is locked to the driver it is stable at the frequency shift Δ_{dm}. When the ILM is near an impurity mode and $0 < \Delta_{di} < \Delta_{dm}$, attraction occurs. In that case, the ILM releases some amplitude and becomes trapped at the impurity site. When the impurity is removed, the ILM amplitude is recovered.

A sudden application of an impurity may end up un-locking the driver from the ILM and it will disappear in an energy dissipation relaxation time. To maintain the locked ILM its change in amplitude should occur over a longer time interval than the damping time.

In this report we show with simulations that an inhomogeneous, harmonic force constant, time dependent perturbation applied to a nonlinear lattice can be used to control ILMs that are locked to a driver. Such manipulation produces logic operations. All logic operations such as addition, subtraction, etc can be made from basic sets of gates called complete sets. Complete sets are (i) NAND and (ii) NOR gates, but (iii) the combination of OR and EXOR gates, of interest here, also form a complete set.[3] By application of the disturbance to the micromechanical cantilever array an inverter and EXOR-NOT operation are demonstrated.

2. Inversion

Our micro-mechanical array simulation model is based on the experimental observations for cantilever arrays described in Ref. [1]. It makes use of the lumped element model equation for cantilever i:

$$\begin{aligned} & m_i\ddot{x}_i + \frac{m_i}{\tau}\dot{x}_i + k_{2Oi}x_i + k_{4O}x_i^3 \\ & + \sum_j k_{2I}^{(j)}(2x_i - x_{i+j} - x_{i-j}) \\ & + k_{4I}[(x_i - x_{i+1})^3 + (x_i - x_{i-1})^3] = m_i\alpha\cos\omega_d t \end{aligned} \qquad (1)$$

where m_i is the mass, τ is a life time, k_{2Oi} and k_{4O} are onsite harmonic and quartic spring constants, $k_{2I}^{(j)}$ is a harmonic intersite spring constant of j-th nearest neighbor, k_{4I} is a quartic intersite spring constant, α is an acceleration , and ω_d is the driver frequency. The array is made from an alternative sequence of long and short cantilevers to insure coupling to the optic branch with the uniform acceleration force provided by a PZT transducer. Thus, m_i and k_{2Oi} are alternatively repeated along the array. The nonlinear components k_{4O} and k_{4I} are both positive and $k_{4I} \gg k_{40}$. The ILM is generated above the highest linear resonant band frequency (137.1kHz). The center of the ILM is at the short cantilever site (odd number site in the simulation).

The lattice disturbance is introduced as a time and spatial dependence of the onsite harmonic spring constant over a fixed region. The spatial pattern to be applied to the

array is shown in Fig. 1(a). It extends over a third of the lattice and the maximum increase in the onsite harmonic spring constant is 10%. As shown in Fig. 1(b) at the time of maximum application the top 16 modes range from extended island modes at low frequencies to local modes at high frequencies.

Figure 2(a) shows a simulation result for the time dependence of a locked ILM in the presence of the time-dependent spatial disturbance. The driver frequency is fixed at 139.0 kHz, so $\Delta_{dm} = 1.9\,\mathrm{kHz}$ while $\Delta_{di} = 0.05\mathrm{kHz}$ at the disturbance maximum. After turning the disturbance on instantaneously a localized pulsing structure appears at its center, indicating an amplitude modulation (AM) of the trapped ILM. Upon reducing the strength of the perturbation to 0 in a time characterized by the ILM relaxation time, τ , one ILM remains in the system. The presence or absence of the ILM depends crucially on the phase of its AM modulation at the time of the removal of the disturbance. Fig. 2(b) shows that if the removal of the disturbance is one half period AM earlier than for frame (a), no ILM remains. At least three cycles of "presence" and "absence" of ILMs are seen in simulations when the removal time is scanned with respect to the AM period. The difference in the end results, i.e., ILM or no ILM, is observed in the time region where the pulsing structure is clearly seen.

Figure 2(c) shows an ILM at site 87 interacting with a disturbance whose growth and removal time is the same, $\sim \tau$. In this case the initial ILM is attracted to island modes of larger and larger amplitude shifting it towards the local mode at center of the disturbance (site 111). Notice the interesting result that the ILM crosses the disturbance center due to its translational inertia and oscillates about that "equilibrium" position. At the same time, the AM of the nonlinear mode at the disturbance center begins to grow in amplitude. This nonlinear mode is an incipient ILM that stabilizes once the disturbance is removed, similar to that shown in Fig. 2(a). At a later time (around 6000~7000 periods) the phase of the AM is shifted by 180 degrees compared with it value in Fig. 2(a). Since the phase is inverted, the end result is also inverted even if the removal time interval of the disturbance is unchanged. It should be noted that the combination of the translation and the AM with respect to the time disturbance causes the results shown in Fig. 2(c) to depend to some extent on the initial relative location of the ILM.

The first two frames in Fig. 2 have also been obtained in another set of simulations where the time dependent pattern shown at the bottom of Fig. 2(c) is used. In this case the time dependence of the disturbance is the same in frames (a) and (c) with its finish shifted by 1/2 period in (b). As expected the AM patterns are the same between t = 4000~6000 periods in (a) and (b), while the pattern is inverted in (c) as illustrated by the vertical arrows shown in all three frames. The 180 degree phase shift of the amplitude modulation in (c) causes the end result to be reversed from that in (a). It is the presence and location of the initial ILM that changes the result. Assigning the existence and absence of ILMs as "1" and "0", the simulations described here demonstrate inverter action in the array.

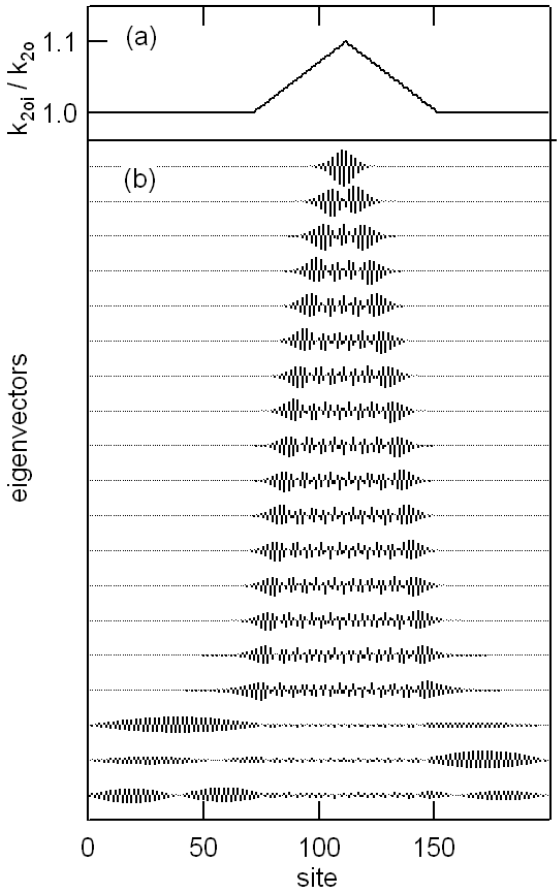

Figure 1. (a) Spatial inhomogenous pattern applied to manipulate ILMs. The disturbance is characterized as the ratio of the on-site impurity spring constant to the pure one. (b) Linear eigenvectors from the highest resonance frequency down to the 19-th mode. The top 16 modes show a variety of localization behavior. Extended band modes begin at the 17-th mode.

3. EXOR-NOT operation

Figure 3(a) shows that when the initial ILM is located on the symmetrically opposite side of the disturbance, at site 135, and the same time dependence of Fig. 2(c) is applied, the AM of the ILM is inverted. When two ILMs are placed at sites 87 and 135 then at the end of the perturbation cycle one ILM remains as shown in Fig. 3(b). In this case, the smooth AM observed in Fig. 2 (a) is more difficult to see.

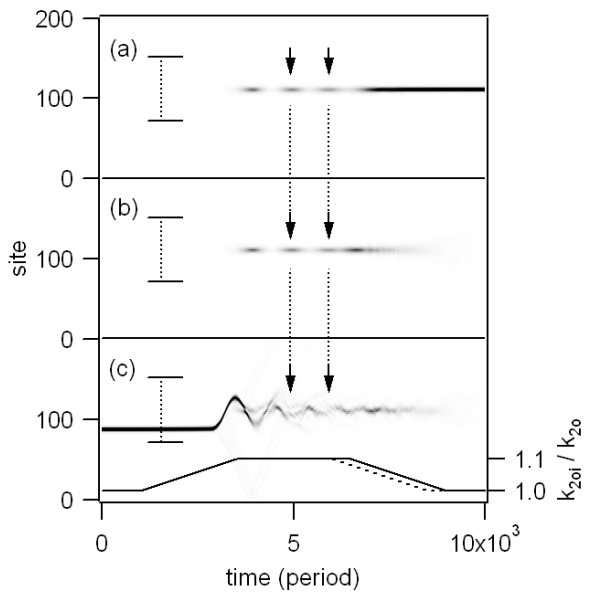

Figure 2. Simulated inverter logic in a micromechanical cantilever array. Dark region corresponds to high energy. The horizontal lines separated by a vertical dashed line identify the boundaries of the triangular disturbance. (a) One ILM is created from the no ILM state. (b) If the disturbance is removed a half AM period earlier than (a), see dashed line in (c), no ILM remains. (c) ILM at site 87, shifted by 24 units from the maximum, is destroyed by the lattice perturbation. The solid line shows the time dependence of disturbance used in (a) and (c). Vertical arrows indicates different times where energy has peaks in (a).

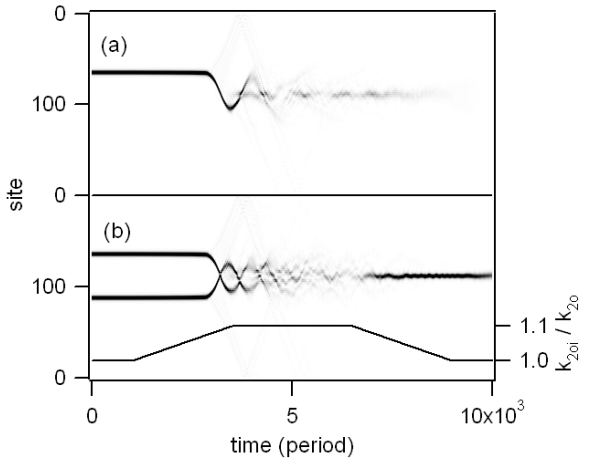

Figure 3. EXOR-NOT logic operation. (a) Initial ILM at site 135, shifted by 24 sites to the other side of the disturbance maximum. (b) Two simultaneous ILMs at site 87 and site 135 give rise to a single ILM after the perturbation is applied and removed.

Table I. Truth table of the logic operation. A and B are inputs at sites 135 and 87. Output site is 111. "1" and "0" mean existence and absence of ILMs. From this table, we can see that the logic operation $\overline{A}\overline{B} + AB$ is realized. It corresponds to the EXOR-NOT.

A(135)	B(87)	Output(111)	Figure
0	0	1	2(a)
0	1	0	2(c)
1	0	0	3(a)
1	1	1	3(b)

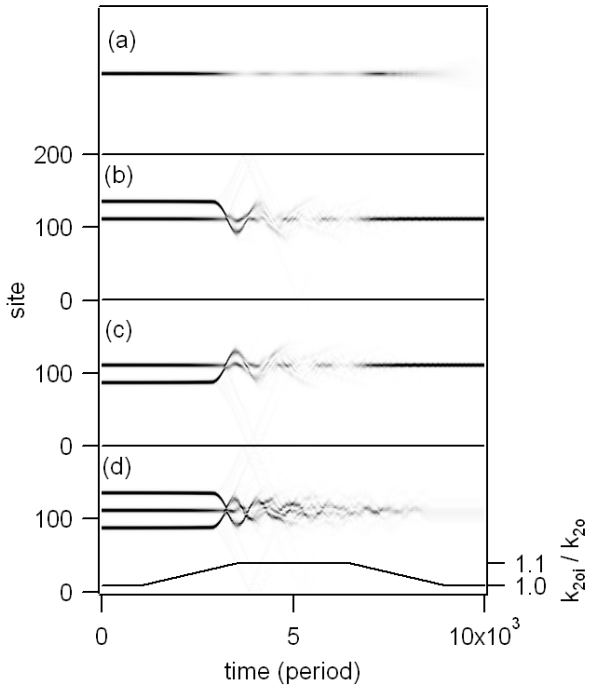

Figure 4. Three inputs logic operation. Spatial pattern and time dependence of the disturbance are the same for all cases. Only the initial conditions are different.

We can make a truth table for the triangular disturbance operation. Inputs are the initial existence or absence of ILMs at sites 87 and 135. The output is site 111, the peak of the impurity pattern in Fig. 1. The results from Figs. 2 and 3 are summarized in Table I. Output "1" is obtained for inputs "00" or "11". The operation is expressed as $\overline{A}\overline{B} + AB$ and it is EXOR-NOT.

If the logic "0" results for two ILMs placed at other symmetric distances with respect to the disturbance center then logic operations are still possible as long as the "0" occurs with high reliability. In this case, the 3rd column, last row of the truth table will be changed to "0" and the operation expression will be $\overline{A}\overline{B} = \overline{(A+B)}$, that is, a NOR gate. For all operations observing a well-defined AM is most important.

4. Three inputs

Since the spatial width of the perturbation is much larger than the width of a single ILM, multiple ILMs can interact with this disturbance. Figure 4 provides such an example. In Fig. 4(a) the initial ILM is placed at site 111 (the center of the disturbance**);** afterwards no ILM remains. Figures 4(b) and 4(c) show two ILMs placed at site 111 and site 87 (or 135); the end result is one ILM. Figure 4(d) illustrates that the interaction with all three produces no ILMs. Combining all of the results shown in Figs. 2, 3, and 4, the output is "1" only when two inputs are "1" and the remaining input is "0".

Note that finding a unique dynamical path for the three input case may be relatively difficult compared to the condition for the two input logic operation where simulations nearly always end in a systematic way. If the process is too sensitive to the initial conditions, the result is largely controlled by noise.

5. Discussion

Two transient phenomena have been observed in the production or destruction of an ILM. The oscillation of the ILM around the point of maximum disturbance indicates the ILM has translational inertia. The other effect, the transient AM is more difficult to explain.

For a linear oscillator the AM frequency is the difference frequency between the driver and the oscillator, i.e., $\Delta_{di} = 0.05\,\mathrm{kHz}$, but the observed AM oscillation frequency is ~0.14 kHz. In addition, the lifetime of the AM (~2300 periods) is longer than the damping time, τ~1200 periods. Thus, the AM cannot be explained by a simple linear calculation**,** instead it must be strongly influenced by the nonlinear effect.

Such AM has already been observed in the sideband spectrum of driver locked ILMs[4] and has been identified with a low frequency deformation mode of the ILM itself.[5] The oscillation parametrically receives energy from the main driver so this parasitic oscillation has a longer lifetime than for the linear case. The added translational component observed here may be the source of the large AM depth.

Bistability of a driver locked ILM is a known property. [6] and such bistability is also known to occur for a Duffing oscillator. By using the ILM eigenvector and a transformation method described in Ref. [7] a Duffing model has been created with effectively the same parameters as used in the above simulations. Similar to the array case, locked and unlocked final states appear alternatively when the perturbation removal time is changed by 1/2 the AM period. Thus, one nonlinear oscillator with a fixed driver is sufficient to have both amplitude modulation and two end results, namely, locked and un-locked states.

Even if amplitude oscillation and bistability are explained by the single nonlinear oscillator model, the multiple input operation demonstrated here requires many degrees of freedom. Since the end result is sensitive to the phase of the AM of the ILM, logic operations are possible as long as a method to modify its phase can be found.

6. Summary

Logic operations inverter and EXOR-NOT have been demonstrated in simulations involving a cantilever array. The triangular spatial perturbation operated off-center to the initial ILM state inverts the existence or absence of the ILM. The operation is explained by a phase shift of the AM produced by the attraction of the initial ILM(s) and the growing (or decaying) array of impurity modes produced by the time dependent perturbation. Any kind of logic operations can be achieved by combinations of the inverter and EXOR-NOT.

The operations shown here are based on the transient response AM together with the bistability of this Duffing-like oscillator. Such a process also would be expected to occur in other kind of MEMS oscillator arrays. Finally, such logic operations may be applicable to information processing, actuator arrays, and sensor arrays[8, 9].

References

[1] M. Sato, B. E. Hubbard, and A. J. Sievers, Nonlinear energy localization and its manipulation in micromechanical oscillator arrays, Rev. Mod. Phys. **78**, 137 (2006).

[2] M. Sato, S. Yasui, M. Kimura, T. Hikihara and A. J. Sievers, Management of localized energy in discrete nonlinear transmission lines, Euro Phys. Lett. **80**, 3002(2007).

[3] S. L. Hurst, "The Logical processing of Digital Signals", Chap. 1 (Crane, Russak & Company, Inc., New York, 1978).

[4] M. Sato, B. E. Hubbard, L. Q. English, A. J. Sievers, B. Ilic, D. A. Czaplewski, H. G. Craighead, Study of intrinsic localized vibrational modes in micromechanical oscillator arrays, Chaos **13**, 702 (2003).

[5] M. Sato, B. E. Hubbard and A. J. Sievers, to be published.

[6] T. Rossler and J. B. Page, Intrinsic localized modes in driven anharmonic lattices with realistic potentials, Physics Letters A **204**, 418 (1995).

[7] M.R.M. Crespo da Silva and C.C. Glynn, Nonlinear Flexural-Flexural-Torsional Dynamics of Inextensional beams II. Forced motions, J. Struct. Mech. **6**, 449 (1978).

[8] M. Spletzer, A. Raman, H. Sumali, and J. P. Sullivan, Highly sensitive mass detection and identification using vibration localization in coupled microcantilever arrays, Appl. Phys. Lett. **92** 114102 (2008).

[9] J. Wiersig, S. Flach and K.-H. Ahn, Discrete breathers in ac-driven nanoelectromechanical shuttle arrays, Appl. Phys. Lett. **93**, 222110 (2008).